Visual introduction to Gaussian beams using a single lens as an interferometer

J. Peatross and M. V. Pack

Visual introduction to Gaussian beams using a single lens as an interferometer

J. Peatross and M. V. Pack
Department of Physics and Astronomy, Brigham Young University, Provo, Utah 84602-4604

Weak surface reflections from a simple lens can be used to observe interferences between collimated and focusing laser beams. The superimposed beams (one resulting from a double reflection within the lens) can be made to have similar intensities near the focus of the weaker beam by choosing the lens prescription and the divergence of the incident laser. An advantage to this inexpensive setup is its stability against vibrations. The relative phase between the two beams can be easily controlled through small adjustments to the lens alignment. Students using this setup with a CCD camera can explore the amplitude and phase properties of a Gaussian laser beam in the vicinity of the focus. This article also includes a brief review of Gaussian beams in the context of the Fresnel diffraction. © *2001 American Association of Physics Teachers.*

I. INTRODUCTION

In this article, we present an experimental setup for introducing students to Gaussian laser beams. We also review the Gaussian laser field in the context of Fresnel diffraction theory.[1–4] Although the expression for the laser field is somewhat complicated, each component of the expression has a clear physical interpretation and can be explored by students using a simple interferometric setup. Others[5,6] have previously discussed the educational benefits of analyzing a focusing laser beam, especially when interferometrically superimposed with a collimated beam. Such a superposition can be realized with a Michelson or Mach–Zehnder-type interferometer setup.[5] The interference between the two beams reveals the form of the field. However, the interference pattern can suffer from vibrational jitter in these types of setups, especially if mechanical components are subject to stringent cost restraints.

In this article, we show how a single lens can be used to produce a superposition of a collimated and a focusing laser beam. This simple and inexpensive "interferometer" has essentially no path-delay jitter, while the phase between the two beams can be controlled easily through subtle adjustments to the tilt of the lens. The lens is positioned in a diverging beam such that after passing through the lens the beam is collimated. A reflection from the back lens surface followed by a reflection from the front surface produces a weak second beam which also travels in the forward direction (referred to as a ghost beam). Since this double reflection in the lens involves only a small fraction of the beam power, it is possible to make the two beams have the same intensity in the region where the ghost beam is focused (with appropriately chosen parameters). This results in an interference pattern with optimal visibility. A CCD camera can be used to view this interference pattern created by the two beams.

II. FRESNEL DIFFRACTION OF A GAUSSIAN PROFILE

Physics undergraduates often study scalar diffraction theory as part of a traditional upper-division optics course. Most diffraction problems (e.g., typical homework problems) are executed in the Fraunhofer limit since there are few aperture geometries for which the full Fresnel–Kirchhoff integral can be performed analytically. The Fresnel approximation to the diffraction integral is appropriate over a much wider range of distances including the Fraunhofer limit, but again there are few problems for which the Fresnel integral can be performed analytically with a finite aperture. For example, Fresnel diffraction from a circular or rectangular aperture can only be solved numerically or with the help of arcane tools such as the Cornu spiral.

A Gaussian field profile *can* be solved analytically within the Fresnel approximation. This problem is pedagogically important not only because it can be carried out to completion, but also because it describes the profile of common single-mode laser beams. This is of practical benefit since a significant fraction of students will at some point require an understanding of laser beam focusing characteristics for research or engineering applications. Of course a good treatment of Gaussian laser beams is available in some optics textbooks,[3,7] as well as in books on laser physics.[1,2,4,8,9] However, the treatment is traditionally presented in the context of finding solutions to the scalar Helmholtz equation under the paraxial approximation. The fact that the Fresnel diffraction integral satisfies the scalar paraxial Helmholtz equation is only occasionally emphasized,[1,2,4] and students can miss the connection between Gaussian optics and Fresnel diffraction, namely, the fact that they are one and the same. Many optics text books,[10–12] which introduce Fresnel diffraction, do not consider the Gaussian aperture.

In a course that addresses a large variety of optical topics within a semester, Gaussian beams can be introduced naturally as a straightforward Fresnel diffraction integral problem. This economizes topics since Fresnel diffraction is seemingly obligatory in a standard optics course, whereas the generation of solutions to the paraxial wave equation might be appropriately addressed in a separate laser course. A treatment of higher-order modes or the ABCD law for Gaussian beams might also be left to a separate course in laser physics. Nevertheless, for the majority of students, a basic understanding of a lowest-order-mode Gaussian beam is an insightful (and perhaps essential) part of an undergraduate education.

We will briefly summarize the well-known Fresnel diffrac-

tion integral applied to a Gaussian field profile. Although the resulting expression is somewhat cumbersome, we find that students are able to arrive at the result when the form of the answer is specified and if a suitable ''integral table'' is provided. While it is important for students to appreciate the result theoretically as an application of Fresnel diffraction, an experimental analysis of the formula makes it much more meaningful.

Let a monochromatic field distribution in the plane $z=0$ be specified by

$$E(x',y')=E_0 e^{-(x'^2+y'^2)/w_0^2}, \qquad (1)$$

where w_0 represents the size of the beam waist. We assume that the field propagates in the $+z$ direction. The Fresnel diffraction integral for finding the field in any location is given by

$$E(x,y,z)=-i\frac{e^{ikz+i(k/2z)(x^2+y^2)}}{\lambda z}\int_{-\infty}^{\infty}dx'\int_{-\infty}^{\infty}dy'$$
$$\times E(x',y')e^{i(k/2z)(x'^2+y'^2)}e^{-i(k/z)(xx'+yy')}. \qquad (2)$$

The integrals in the x and y dimensions are performed with the aid of

$$\int_{-\infty}^{\infty}e^{-Ax^2+Bx+C}\,dx=\sqrt{\frac{\pi}{A}}e^{(B^2/4A)+C}, \quad \text{Re}\{A\}>0. \qquad (3)$$

Alternatively, the integrals can be executed in cylindrical coordinates resulting in the following Hankel transform:[13]

$$\int_0^{\infty}\rho e^{-\alpha\rho^2}J_0(\beta\rho)\,d\rho=\frac{e^{-\beta^2/4\alpha}}{2\alpha}, \quad \text{Re}\{\alpha\}>0. \qquad (4)$$

The algebra involved in arriving at the final form can be intimidating for some students (and time consuming). It may therefore be appropriate to provide some steps in the algebra along with the necessary integral formula. In any case, the mechanics of performing the operations is of secondary importance compared to an appreciation of Eq. (2) and an intuitive grasp of the result. The standard form of the result is[1,4]

$$E(\rho,z)=E_0\frac{w_0}{w(z)}e^{-[\rho^2/w^2(z)]}e^{ikz+i[k\rho^2/2R(z)]-i\tan^{-1}(z/z_0)}, \qquad (5)$$

where

$$w(z)\equiv w_0\sqrt{1+z^2/z_0^2}, \quad R(z)\equiv z+z_0^2/z, \quad z_0\equiv kw_0^2/2.$$

Here ρ is the usual radius $\sqrt{x^2+y^2}$ given in cylindrical coordinates.

III. USING A LENS TO CREATE BEAM SUPERPOSITION

To appreciate Eq. (5), ideally students should study a laser beam with a CCD camera. If a single beam is analyzed, the rich phase structure of the field is not seen, but rather only its intensity:

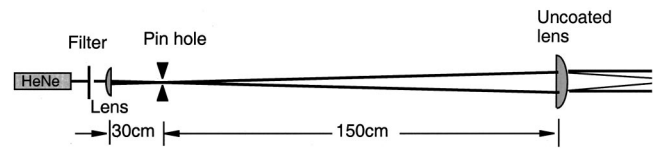$$I_1(\rho,z)=I_0\frac{w_0^2}{w^2(z)}e^{-[2\rho^2/w^2(z)]}. \qquad (6)$$

Fig. 1. Experimental setup for creating a superposition of a collimated and a focusing beam.

However, if the beam is superimposed with a plane wave $E_2 e^{ikz-i\phi}$, where ϕ is a constant relative phase term, then the intensity for the combined fields is

$$I_t(\rho,z)=\left[I_2+I_1(\rho,z)+2\sqrt{I_2 I_1(\rho,z)}\right.$$
$$\left.\times\cos\left(\frac{k\rho^2}{2R(z)}-\tan^{-1}\frac{z}{z_0}+\phi\right)\right]. \qquad (7)$$

(I_2 is the intensity of the reference plane wave alone.) In this case, the effects of the wave front radius of curvature $R(z)$ and the Gouy shift $-\tan^{-1}z/z_0$ are seen in the interference pattern.

The arrangement of two collinear fields, one collimated and one converging, constitutes the classic Gouy experiment. The main emphasis of the present article is to present a simple idea for creating this superposition using a single lens. The overall experimental setup that we have used is shown in Fig. 1. A relatively wide collimated beam is created using a telescope. This provides an adequate representation for the plane wave field. Internal reflections within the final lens provide the superimposed converging field (ghost beam). A long focal length lens is ideal for the second end of the telescope so that the ghost beam does not focus too sharply. In our case, the light was collimated using a plano-convex lens with a 150 cm focal length. We placed a 1 mm pinhole in the telescope to clean some of the spurious light in our laser beam; the use of the pinhole is not critical. A laser with good mode quality and a significant coherence length (a few centimeters or greater) is necessary, a HeNe laser being a good choice, which is what we used.

Figure 2 illustrates how a ghost beam is formed in the exit lens of the telescope. The effective focal length of the final lens in the case of the light undergoing the double reflection may be found (within the thin-lens approximation) by multiplying the ABCD matrices for entry into the flat lens surface followed by reflection from the curves surface and finally transmission through the curved surface:
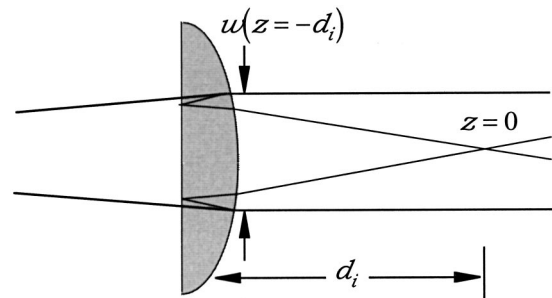

Fig. 2. Focusing beam created from a weak reflection from the second surface followed by a weak reflection from the first surface.

$$\begin{pmatrix} 1 & 0 \\ -(n-1)/R & n \end{pmatrix} \begin{pmatrix} 1 & 0 \\ -2/R & 1 \end{pmatrix} \begin{pmatrix} 1 & 0 \\ 0 & 1/n \end{pmatrix}$$

$$= \begin{pmatrix} 1 & 0 \\ -(3n-1)/R & 1 \end{pmatrix}. \tag{8}$$

The effective focal length of this system is seen to be

$$f_{\text{eff}} = \frac{R}{3n-1} = \frac{n-1}{3n-1} f, \tag{9}$$

where f is the focal length of the lens in the usual sense. In the above example, we assumed a plano-convex lens, but Eq. (9) is in fact valid for the double-reflection ghost beam transmitted through any thin lens.

In our setup, we used an uncoated lens which reflects about 4% of incident power at each surface. Thus, after two reflections, the ratio of the power carried by the ghost beam to that carried by the collimated beam is about $r_{\text{power}} = 0.16\%$. However, near its focus the power in the ghost beam is concentrated, which compensates for this factor, making the intensities of the two beams similar. To compare the strength of the two fields in the vicinity of the ghost beam focus, it is necessary to compute the relative sizes of the two beams. Let the distance from the lens to the ghost beam focus be d_i, as depicted in Fig. 2. The ghost beam waist at $z=0$ (at a distance d_i after the lens) may be viewed as an image of the beam waist inside the telescope located at a distance $d_0 = f$ before the lens. This distance is connected to the (effective) focal length of the lens via the usual imaging relation

$$\frac{1}{f_{\text{eff}}} = \frac{1}{d_0} + \frac{1}{d_i} \Rightarrow d_i = \frac{n-1}{2n} f. \tag{10}$$

(In our case, this imaging relation agrees with the ABCD law for Gaussian beams to within 4%, and so it is quite adequate for obtaining the approximate location of the ghost beam waist; one finds the exact location with the CCD camera.) For our setup, and taking the refractive index to be approximately $n = 1.5$, the distance to the ghost beam focus turns out to be approximately $d_i = 25$ cm.

The radius of the ghost beam at its focus is

$$w_0 = \frac{2\lambda f^{\#}}{\pi}, \tag{11}$$

where the f number is the ratio d_i to the diameter of the beam at the lens [i.e., $2w(-d_i)$] which is the same as the diameter of the collimated beam over a long range after the lens. In our case, the diameter of the collimated beam was chosen to be $2w(d_i) = 2.5$ mm, measured with the CCD camera as seen in Fig. 3. This is adjustable through an appropriate choice of focal length and position of the lens on the front end of the telescope. The f number for the ghost beam in our case is $f^{\#} = 100$, corresponding to a beam waist radius of $w_0 = 40$ μm (with the wavelength $\lambda = 633$ nm). This tiny spot is also visible in Fig. 3. To find the relative intensity between the two beams at $z=0$ (i.e., the ghost beam focus), we must compare the squares of $w(\pm d)$ and w_0, which are proportional to the respective beam areas. For our setup, the area ratio is $r_{\text{area}} = w_0^2/w(\pm d)^2 = 0.10\%$. This means that the ratio of intensities in the vicinity of the ghost beam focus is $I_1((0,0)/I_2 = r_{\text{power}}/r_{\text{area}} = 1.6$, which leads to reasonably
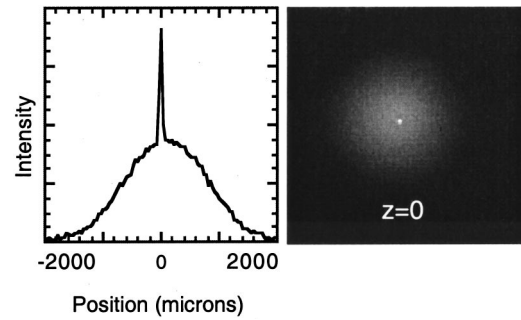

Fig. 3. Intensity profile of the ghost beam at its focus inside the collimated beam.

good fringe visibility in the interference pattern. While the larger collimated beam does vary in intensity as a function of radius (as seen in Fig. 3), we can treat it as a plane wave in Eq. (7) since the interference with the ghost beam takes place in a relatively localized region over which the collimated beam is nearly uniform.

IV. MEASUREMENTS AND ANALYSIS

This stable interferometer setup allowed us to study the amplitude and phase properties of the ghost beam directly with a CCD camera. To adjust exposure to the CCD camera, filters were placed in the beam before the telescope. Figure 4 shows the intensity on the camera as a function of radius at various values of z. With subtle adjustments to the tilt of the lens, it is possible to control the relative phases of the two beams. For these curves, the phase has been set approxi-
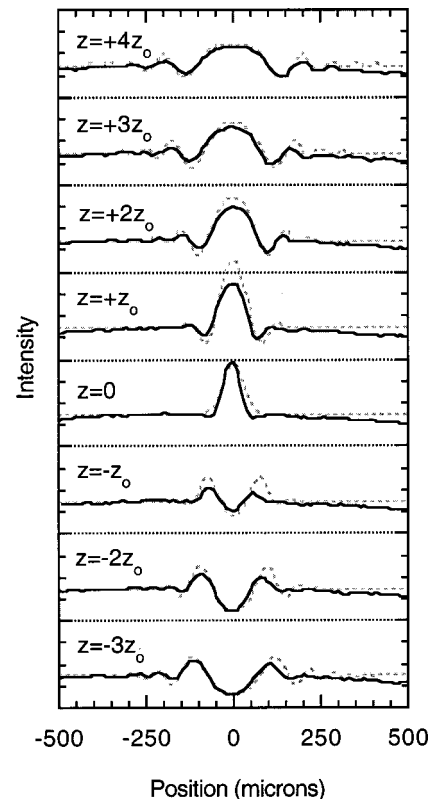

Fig. 4. Intensity curves showing the interference between the ghost and collimated beams both measured (solid) and theoretical (dotted).
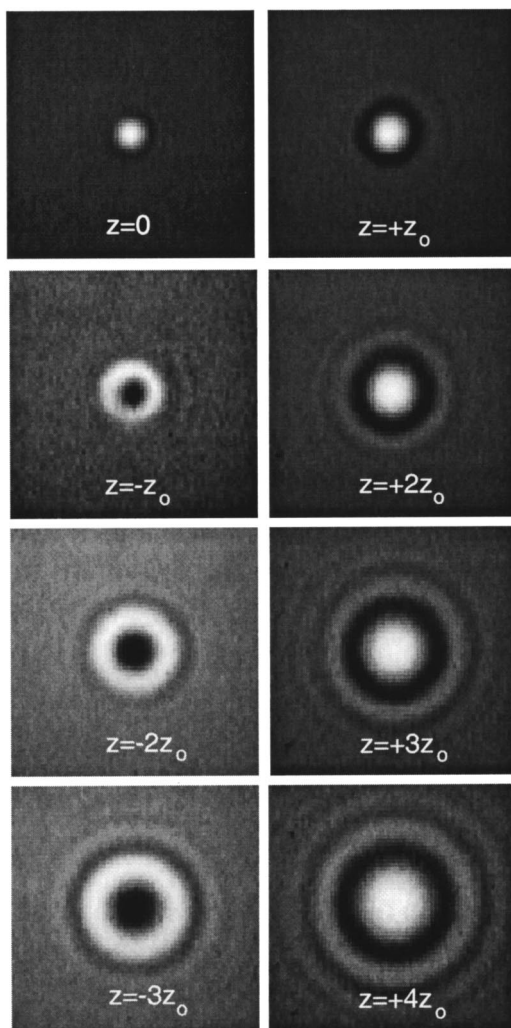
Fig. 5. Images showing the interference between the ghost and collimated beams in the region of the focus. The pixel size on the camera is 9.6 μm $\times$ 9.6 μm.

mately to $\phi = \pi/2$. In this case the interference term in Eq. (7) vanishes at the focal plane, and the total intensity at that plane is the sum of the intensities of the individual beams. Therefore, the curve for $z = 0$ is roughly that of a focused beam on top of a uniform background. The dotted curves in each case are the theoretical predictions of Eq. (7). We fit the formula to the measurement at $z = 0$; we held the parameters fixed for other frames. Some discrepancy near $z = \pm z_0$ may be due to ϕ being slightly out of adjustment from $\pi/2$; ϕ was not adjusted as a parameter in the fit.

The radius of curvature $R(z)$ is responsible for the interference fringes as a function of radius ρ. The distribution of these ring patterns is in agreement with the predictions of Eq. (7). At the focus, the radius of curvature $R(0)$ is infinite so that no ring pattern is present. The smallest radius of curvature and therefore the tightest ring pattern occurs at $z = \pm z_0$. However, at this distance ($z_0 = 8$ mm in our case) the beam is contained mostly within the ring pattern, making

fringes difficult to see unless the intensity of the ghost beam is much greater. This makes it difficult to accurately extract z_0 from the radii of the fringes. The Gouy shift $-\tan^{-1} z/z_0$ gives rise to an interference which enhances the on-axis intensity after the focus and diminishes the on-axis intensity before the focus.

Figure 5 shows a sequence of images similar to the ones used to generate Fig. 4. However, for theses images the f number in the telescope (and hence also in the ghost beam) was adjusted slightly to increase the relative intensity of the ghost beam at its focus to roughly 4 times the intensity of the collimated beam. This improved the fringe visibility of the rings well away from the focus. Each frame shows an area 640 μm$\times$640 μm. The fact that the ring patterns before and after the focus are inverted is a direct manifestation of the Gouy shift.[14]

V. SUMMARY

We have used this new single-lens interferometer in a classroom setting. Our experience with using it as an instructional tool has been very positive. Previously, we had used a more traditional interferometer setup (modified Michelson configuration) to create a superposition of two laser beams, but the jitter and drift in the fringe pattern made quantitative study very difficult for students (using our hardware). For example, when viewing evidence of the Gouy shift, the fringe pattern might reverse (drift in phase by π) in the time it takes to make observations before and after the focus. With the single-lens interferometer, however, this problem has been completely eliminated; the fringe pattern remains stable for hours.

[1] O. Svelto, *Principles of Lasers* (Plenum, New York, 1998), 4th ed., pp. 145–156.
[2] P. W. Milonni and J. H. Eberly, *Lasers* (Wiley, New York, 1988), pp. 519–523.
[3] M. V. Klein and T. E. Furtak, *Optics*, 2nd ed. (Wiley, New York, 1986), pp. 468–474.
[4] A. E. Seigeman, *Lasers* (University Science Books, Mill Valley, CA, 1986), pp. 630–640.
[5] P. Nachman, "Mach–Zehnder interferometer as an instructional tool," Am. J. Phys. **63**, 39–43 (1995).
[6] A. M. Almeida, E. Nogueira, and M. Belsley, "Paraxial imaging: Gaussian beams versus paraxial–spherical waves," Am. J. Phys. **67**, 428–433 (1999).
[7] R. D. Guenther, *Modern Optics* (Wiley, New York, 1990), pp. 336–343.
[8] Reference 2, pp. 480–490.
[9] K. J. Kuhn, *Laser Engineering* (Prentice Hall, New Jersey, 1998), pp. 83–101.
[10] E. Hecht, *Optics* (Addison-Wesley, Massachusetts, 1998).
[11] G. R. Fowles, *Introduction to Modern Optics*, 2nd ed. (Dover, New York, 1975).
[12] J. R. Meyer-Ardendt, *Introduction to Classical and Modern Optics*, 4th ed. (Prentice Hall, New Jersey, 1995).
[13] I. S. Gradshteyn and I. M. Ryzhik, *Table of Integrals, Series, and Products*, 5th ed. (Academic, San Diego, 1994), formula 6.631.4.
[14] R. W. Boyd, "Intuitive explanation of the phase anomaly of focused light beams," J. Opt. Soc. Am. **70**, 877–880 (1980).